

Ferromagnetism in layered metastable $1T\text{-CrTe}_2$

This content has been downloaded from IOPscience. Please scroll down to see the full text.

2015 J. Phys.: Condens. Matter 27 176002

(<http://iopscience.iop.org/0953-8984/27/17/176002>)

View [the table of contents for this issue](#), or go to the [journal homepage](#) for more

Download details:

IP Address: 168.96.66.157

This content was downloaded on 06/07/2015 at 18:00

Please note that [terms and conditions apply](#).

Ferromagnetism in layered metastable $1T\text{-CrTe}_2$

Daniele C Freitas^{1,2}, Ruben Weht^{3,4}, André Sulpice¹, Gyorgy Remenyi¹, Pierre Strobel¹, Frédéric Gay¹, Jacques Marcus¹ and Manuel Núñez-Regueiro¹

¹ Institut Néel, Université Grenoble Alpes and Centre National de la Recherche Scientifique 25 rue des Martyrs, BP 166, 38042, Grenoble cedex 9 France

² Centro Brasileiro de Pesquisas Físicas, Rua Dr. Xavier Sigaud, 150, Urca, Rio de Janeiro—RJ, Brasil

³ Gerencia de Investigación y Aplicaciones, Comisión Nacional de Energía Atómica (CNEA), Avda General Paz y Constituyentes, 1650 San Martín, Argentina

⁴ Instituto Sabato, Universidad Nacional de San Martín—CNEA, 1650 San Martín, Argentina

E-mail: nunez@neel.cnrs.fr

Received 16 December 2014, revised 21 January 2015

Accepted for publication 4 March 2015

Published 15 April 2015



CrossMark

Abstract

We have synthesized for the first time the metastable compound $1T\text{-CrTe}_2$. We have done its complete structural characterization and measured its magnetization, specific heat and electrical resistivity between 4 and 330 K. We have also performed detailed band structure calculations. We have found that it crystallizes in the CdI_2 structure type and that its electrical resistance follows a metallic behaviour below room temperature. Its magnetization and specific heat curves show that the compound has a transition to a ferromagnetic state at $T_C = 310$ K, with the magnetic moments ordered parallel to the basal plane. From the specific heat measurements and the ferromagnetic solutions obtained from our DFT calculations, we conclude that the ferromagnetism is of itinerant nature.

Keywords: ferromagnets, layered materials, chromium

(Some figures may appear in colour only in the online journal)

1. Introduction

The layered transition metal dichalcogenides have been long studied due to their interesting 2D properties, showing a physics extremely rich and varied. As they can be synthesized with a large number of transition metals, which already have very different properties, they develop a large variety of behaviours. Several reviews were devoted recently to discussing their properties, some of them are [1–3]. We just give here a short enumeration of the most interesting cases. The IV and V group transition metals Ti, Nb, Ta and V dichalcogenides present, for instance, electronically driven phase transitions coupled to commensurate or incommensurate lattice distortions, called charge density waves (CDW) [4]. Some of them show superconductivity or develop it when the CDW is destabilised by pressure or doping. For example, superconductivity develops when the CDW of $1T\text{-TiSe}_2$ is destroyed by doping [5] with Cu or by the application of

pressure [6]. Recently, dichalcogenides of other transition metals groups have yielded new surprises. Superconductivity has been induced by breaking down of orbital ordering in $1T\text{-IrTe}_2$ [7] or by breaking of Te_2 dimers in AuTe_2 [8]. Some of the layered transition metal dichalcogenides develop magnetic ground states, an example being antiferromagnetic $1T\text{-CrSe}_2$ and an unusual orbital Kondo Effect was observed in the related $1T\text{-Cr}_{1-x}\text{V}_x\text{Se}_2$ [9]. It is thus appealing to look into similar materials, either known, but not studied, or by synthesizing new ones, in the search of other systems with interesting new properties. In this work we focused our attention on another Cr dichalcogenide, CrTe_2 , that has not been previously synthesized.

Single crystals of the $1T\text{-CrTe}_2$ were obtained through an indirect synthesis and structural, magnetic, thermal and transport properties were measured. $1T\text{-CrTe}_2$ is metastable, decomposing above 330 K and has a transition to a ferromagnetic state just before it, around 310 K. We also

Table 1. Lattice parameters of $1T$ -CrTe₂ obtained by analysis of the peak position by *fulprof* program.

Compound	a	c	c/a
CrTe ₂	3.7887	6.0955	1.6089

studied the effect of V doping. The analysis of the measured data together with its band structure calculations suggests an itinerant nature for the ferromagnetic order.

The paper is organised as follows. In section 2 we explain the synthesis of the samples, their characterization and their physical properties: magnetization, specific heat and electrical resistivity. In section 3 we present the results of band structure calculations. Section 4 contains the discussion and section 5 the conclusion.

2. Experimental

2.1. Synthesis

As for $1T$ -CrSe₂ [10, 11], $1T$ -CrTe₂ compounds were synthesized indirectly by oxidation of KCrTe₂. The parent compounds were prepared by a molar mixture of the elements, Cr, K, Te and V for the doped samples, under argon atmosphere in a glove box. This mixture was heated to the melting point of both, the alkali element and tellurium and then kept at 900 °C for eight days in an evacuated quartz tube. The tubes were opened in a glove box in order to prevent oxidation. Alkaline atom de-intercalation was then carried out by reacting the parent compounds in solutions of iodine in acetonitrile. These suspensions were stirred for about 1 h, using an excess of iodine. The final product was washed with acetonitrile to remove the iodide formed, filtered and dried under vacuum. A mixture of brilliant dark gray platelets about 3 mm long, 0.3 mm thick and black powders with a metallic luster were obtained.

2.2. Structural characterization

Diffraction patterns of $1T$ -CrTe₂ were recorded on a Bruker D8 diffractometer used at coupled to a low temperature cryostat with Cu $K\alpha$ radiation and transmission geometry. Data were collected between $10^\circ \leq 2\theta \leq 90^\circ$, with a 0.020° step and acquisition times between 6 s and 9 s per point. Lattice parameter (see table 1) were obtained by analysis of the peak positions by *fulprof* program.

The diffractograms are shown in figure 1. We found that $1T$ -CrTe₂ crystallises in the CdI₂ structure type (space group $P\bar{3}m1$, N° 164). In this structure, Cr and Te atoms occupy the Wyckoff positions a (cell origin) and $d = (1/3, 2/3, z)$ with $z \simeq 0.25$, respectively. The Cr atoms are octahedrally coordinated by tellurium and form hexagonal layers sandwiched between two layers of Te atoms (see insert figure 1). Same small traces of Te were found in all the samples. Figure 1 and table 1 show the lattice parameters.

Samples were analysed by energy dispersive x-ray spectroscopy (EDX) in a Zeiss Ultra field-emission gun scanning electron microscope operated at 20 kV. Twenty

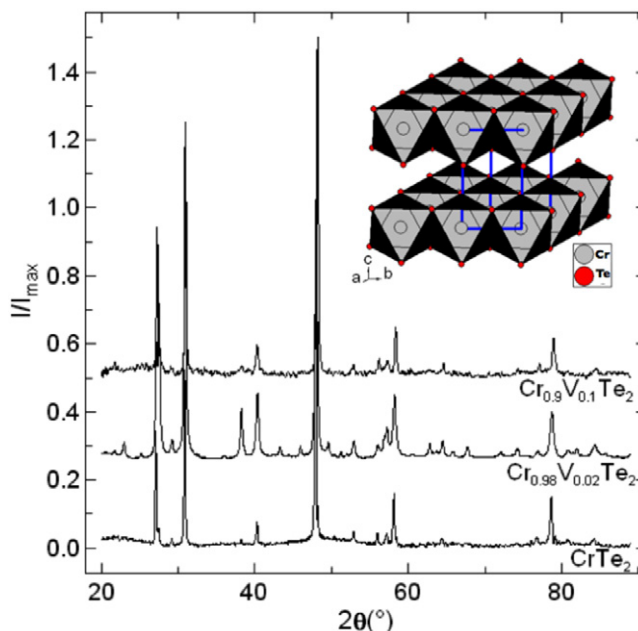


Figure 1. X-ray powder diffractograms of the $1T$ -Cr_{1-x}V_xTe₂ compounds. For better visualization the intensities of the peaks were normalised by the largest peak and the diffractograms were displaced on the vertical scale by 0.5 for each compound. Insert: the schematic 3D structure of $1T$ -CrTe₂. The Te polyhedra centred on the Cr ions are shown. The lines indicate the axes of the unit cell. This figure was generated by DIAMOND 2.1E software [12].

different points were measured from two different regions of the compounds compressed as rectangular bars. The nominal stoichiometry was approximately obtained for different preparations with an excess of environ 5% of metal atoms. We found small quantities of K atoms in all the compounds suggesting that the de-intercalation was not completed.

The lattice parameters were measured by x-ray diffraction of the pure compound in function of temperature as shown in figure 2. The crystallographic transitions [10, 11], contraction of the c parameter and dilatation of the a parameter, found in CrSe₂ was not detected in CrTe₂.

The c parameter falls down monotonically with temperature while the a parameter initially rises to 250 K and then goes down. This dilatation of a -axis is associated with a ferromagnetic order which will be discussed below. As we can see in figure 2 the Cr–Te–Cr angle approaches smoothly 90° below the ferromagnetic transition.

2.3. Magnetization

Magnetization measurements were carried out in a METRON-IQUE Squid Magnetometer in the 1.8–340 K temperature range and a 0–7 T field range. Figure 3 displays the magnetization versus temperature curves under an applied field of 1 kOe for CrTe₂. The magnetization shows a ferromagnetic behaviour which is stronger in the ab plane, unlike the Cr_{1-x}V_xSe₂ which is antiferromagnetic [10]. We were not able to determine the Curie constant in the paramagnetic phase because the ferromagnetic transition is just above ambient temperature. However, at room temperature the crystals were attracted by the tweezers.

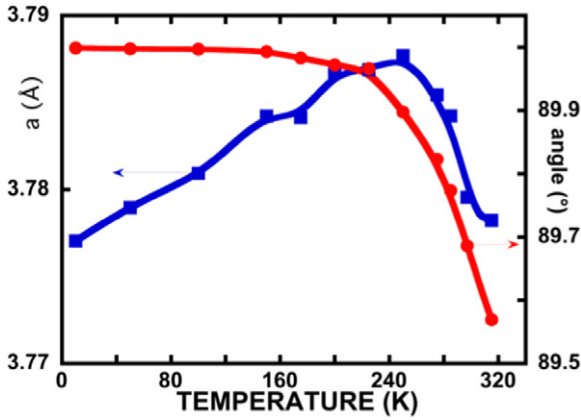


Figure 2. Lattice parameter a and Cr-Te-Cr angle as a function of temperature for CrTe_2 .

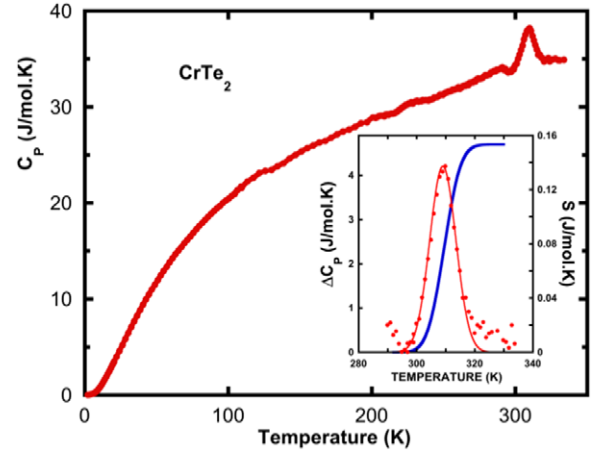


Figure 4. Specific heat of a mono crystal of CrTe_2 . The anomaly seen at $T_C = 310$ K corresponds to the ferromagnetic ordering. Other small anomalies are due to the addenda. Insert: detail showing the specific heat peak without the background and the calculated entropy, than is very small and suggests an itinerant character for the ferromagnetic state.

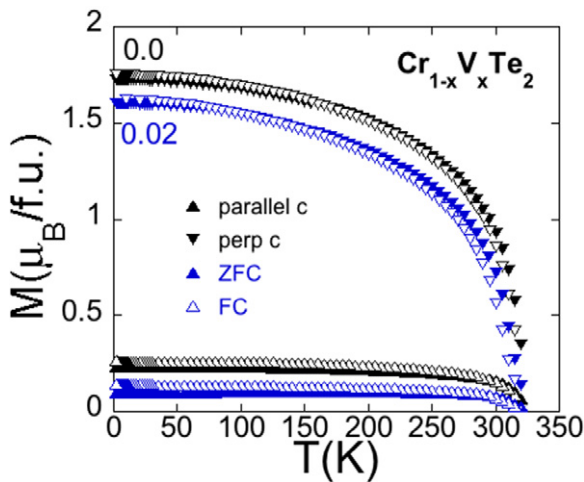


Figure 3. Magnetization of $1T\text{-Cr}_{1-x}\text{V}_x\text{Te}_2$ samples over an applied field of 1 kOe. Zero-field-cooling (empty symbols), ZFC and field-cooling (full symbols), FC, curves show practically no difference with the field aligned perpendicular to c -axis (inverted triangles). For the field aligned parallel to the c -axis (triangles) there is a slight difference between ZFC and FC below 250 K.

2.4. Specific heat

Heat capacity measurements have been performed in the temperature range 1.9–320 K, with the commercial physical property measurement system (PPMS—Model 6000 from Quantum Design Inc.) The PPMS reproducibility of heat pulse relaxation method was 2 per cent. Sample to addenda heat capacity ratio was in general in the same order of magnitude. The sample was attached to the sample holder by a small amount ($m < 0.2$ mg) of Apiezon N grease to achieve a good thermal contact.

The specific heat of a mono crystal of CrTe_2 is shown on figure 4. From the low temperature behaviour, we obtain $\gamma = 13 \text{ mJ mol}^{-1} \text{ K}^2$ and a Debye temperature $\theta_D = 217$ K, values typical of other 2D dichalcogenides [7, 8, 13]. We observe a clear but small peak at about $T_C = 310$ K that corresponds to the ferromagnetic transition. The smaller peak just below in temperature corresponds to the Apiezon grease used for thermalising the sample.

As we do not have any reference baseline, we extrapolate the supposed phonon contribution curve and subtract it from

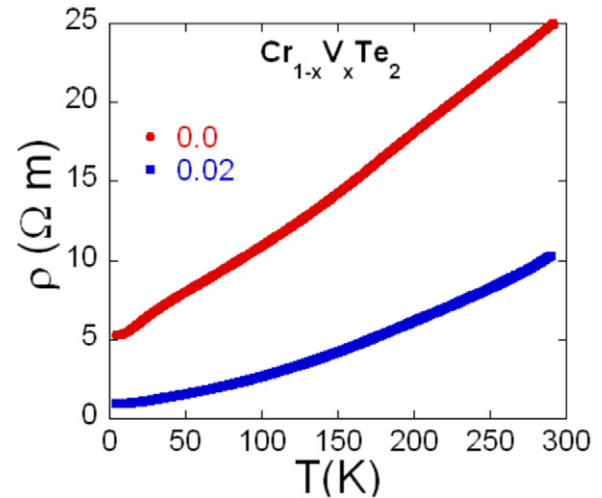


Figure 5. Basal plane electrical resistivity of $1T\text{-Cr}_{1-x}\text{V}_x\text{Te}_2$ mono crystals.

the measured data. The resulting peak is shown in the insert of figure 4, as well as the calculated entropy. The latter is very small, probably implying itinerant ferromagnetism, in contrast to the $R \ln(2)$ expected for localized moments.

2.5. Electrical resistance

The electrical resistance measurements were performed using a Keithley 2400 sourcemeter and a Keithley 2182 nanovoltmeter. Electrical resistance was performed in monocrystals of CrTe_2 . The contacts were done by microwelding of gold wires as the silver epoxy seems to react with samples. The measurements were done in the aligned usual four point contacts disposition, that yields basal plane properties. The resistivity shows a metallic behaviour with temperature, as shown in figure 5 ($\text{RRR} = 5$). There are two slight anomalies at around 150 K and 20 K. They can be attributed to a crystal field effect, but a detailed analysis and the absence of the

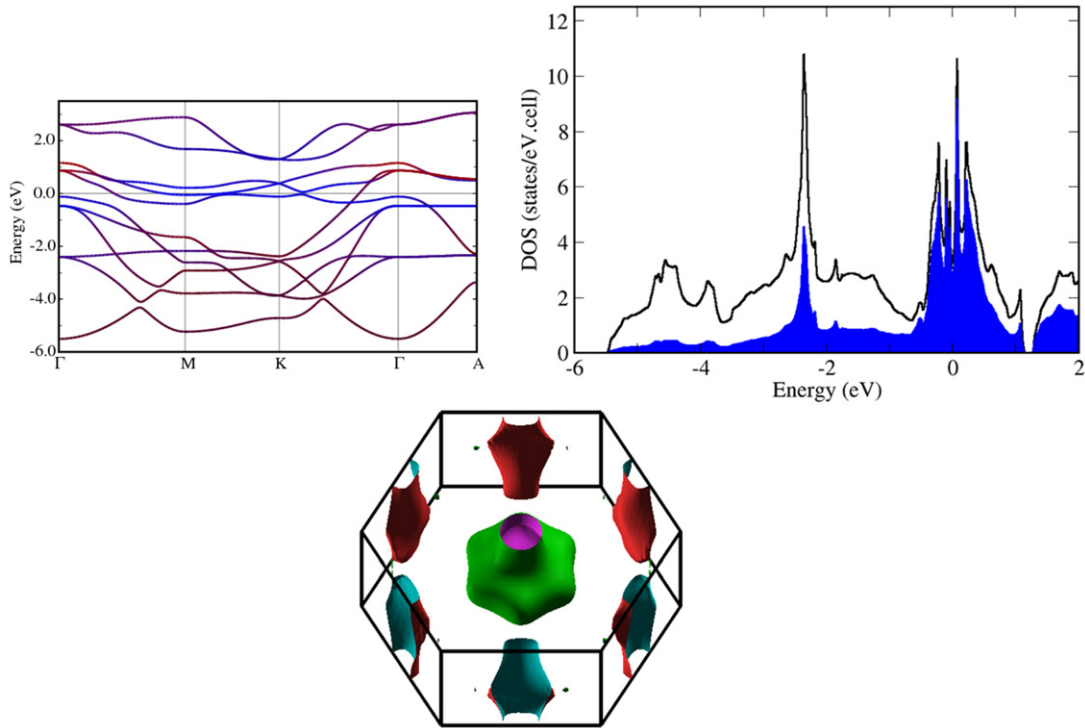


Figure 6. Upper panel: non-magnetic band structure of $1T\text{-CrTe}_2$, blue color: Cr character; red color: Te character. Second panel: density of states also for the non-magnetic configuration. Shadow region shows the Cr character. Third panel: Fermi surface of $1T\text{-CrTe}_2$, showing a hole bellied cylinder with important Te character around the $\Gamma\text{-}A$ line and electron cylinder of mostly Cr character around the $M\text{-}L$ line.

corresponding Schottky anomalies in the specific heat informs such a supposition. More measurements on samples of different batches should be done to clarify the issue. Its sister compound CrSe_2 presents [9], in contrast, an activated electrical resistivity, with small anomalies due to lattice deformations that appear around 150 K. The difference may reside in the semimetallic character of CrSe_2 , that will then be more sensitive to the defects inherent to the indirect method of preparation of the samples.

3. Electronic structure calculations

The electronic properties and energetics of the different magnetic configurations were investigated by electronic structure calculations within the framework of the density functional theory (DFT) [14] and using the Wien2k code [15]. The exchange and correlation potential was considered at the level of the generalised gradient approximation (GGA) based on the Perdew–Burke–Ernzerhof (PBE) expression [16].

As CrTe_2 has a metastable structure, the lattice parameters were kept fixed at the experimental values while the internal positions of the Te atoms were allowed to relax until forces on each atom were below $0.025 \text{ eV \AA}^{-1}$. A value very close to the expected $z \simeq 0.25$ was obtained.

On figure 6 we observe the non-magnetic band structure and density of states. They show the presence of both Te and Cr carriers, with the Cr states strongly dominant around the Fermi level. Those bands are quite flat around the Fermi level showing only a very small dispersion and confirming the two sheets of the Fermi surface. One, centred around the $K\text{-}L$

Table 2. Energy of the different magnetic states with respect to the completely ferromagnetic state (order in the plane—coupling between planes—order in the plane).

State	ΔE (meV Cr^{-1})
NM	800
AF-AF-AF	80
AF-F-AF	76
F-AF-F	19

line in the reciprocal space, formed by almost exclusively Cr orbitals and a second one, a bellied hole cylinder around the $\Gamma\text{-}A$ line, that also has some contribution of the Te orbitals. Although of quite a two-dimensional nature, the Fermi surface does not have any noticeable nesting.

To study the magnetic couplings we have tried different magnetic configurations (table 2) and the most stable is the totally ferromagnetic, whose band structure is shown in figure 7 with their resulting density of states. It is clear that the energy gain is obtained through an approximate Stoner mechanism, splitting the high density of states of the Cr levels in the non-magnetic solution, with a strong lowering of the up Cr bands, while the down Cr bands are shifted well above the Fermi level. This results in a magnetic splitting of around 2–3 eV. Thus, in the ferromagnetic ground state the carriers have a much stronger Te character. As expected, the most important magnetic interaction is within the planes, with a much lower influence between them. However, also in this case a ferromagnetic coupling is preferred. The non-magnetic band structure yields a density of state at the Fermi level

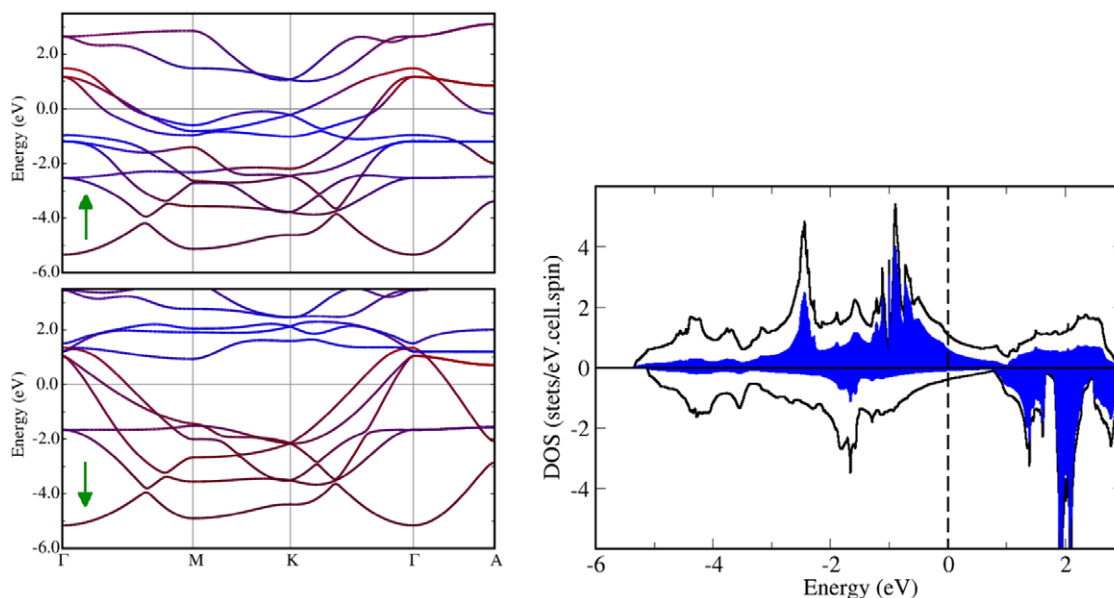


Figure 7. Upper panel: ferromagnetic band structure, showing that ferromagnetic ordering lower the energy of the spin-up bands, while increasing the energy of the spin-down bands. As verified by resistivity measurements $1T\text{-CrTe}_2$ is a conducting semimetal. Lower panel: corresponding density of states.

that corresponds to a $\gamma = 9 \text{ mJ mol}^{-1} \text{ K}^2$ in relatively good agreement with the measured experimental value.

4. Discussion

Studies of the Cr–Se/Te system with different types of replacements have followed the evolution from AF (in Se based compounds) towards F (in Te based materials) [17–22]. $1T\text{-CrTe}_2$ is a compound with a large a parameter and consequently the indirect Cr–Te–Cr exchange of strong ferromagnetic character due to its 90° angle prevails over the direct Cr–Cr exchange of antiferromagnetic character. We note that this analysis would effectively be valid if the Cr^{4+} moments were localized already at high temperature. As we are not able to measure above room temperature due to sample decomposition, this cannot be checked. However, the low value of the transition entropy at T_C as well as the conclusion of the band structure calculations points towards an itinerant ferromagnetic character. Also, the feeble magnetic moment deduced from the magnetization agrees with this picture. Replacement with V expands the c parameter and contracts the a parameter, with clear consequences on the compound’s magnetization. The ratio c/a increases (it approaches the value corresponding to ideal CrTe_6 octahedra) (see figure 2). In the pure compound a dilatation of the a parameter is observed above 250 K that is associated with the ferromagnetic transition (see figure 3). The magnetic moments are aligned parallel to the ab plane as can be inferred by the strong anisotropy of the magnetization. With the V doping the $3d$ ions become closer and the octahedra more regular, i.e. they introduce an AF coupling. This causes the rotation of the magnetic moments out of the ab plane. The magnetization in the c direction is flat for a long range of temperature and does not change with the second transition below 150 K that is assigned by an augmentation of the magnetization in the ab plane.

5. Conclusion

We have synthesized for the first time metastable $1T\text{-CrTe}_2$. The pure compound develops a ferromagnetic ground state around 310 K with moments in the ab plane. Band structure calculations and specific heat measurements show that the ferromagnetism is itinerant. The resistivity shows a metallic behaviour.

Acknowledgments

DCF gratefully acknowledges support from the Brazilian agencies CAPES and CNPQ. RW is fellow of CONICET-Argentina and gratefully acknowledges partial support from CONICET (Grant No. PIP 114-201101-00376) and ANPCyT (Grant No. PICT-2012-0609). We acknowledge clarifying discussions with C Lacroix. We are grateful to S Pairis and O Leynaud for technical help.

References

- [1] Chhowalla M, Shin H S, Eda G, Li L-J, Loh K P and Zhang H 2013 *Nat. Chem.* **5** 263
- [2] Rosnagel K 2011 *J. Phys.: Condens. Matter* **23** 213001
- [3] Xu X, Yao W, Xiao D and Heinz T F 2014 *Nat. Phys.* **10** 343
- [4] Wilson J A, DiSalvo F J and Mahajan S 1975 *Adv. Phys.* **24** 117–201
- [5] Morosan E, Zandbergen H W, Dennis B S, Bos J W G, Onose Y, Klimczuk T, Ramirez A P, Ong N P and Cava R J 2006 *Nat. Phys.* **2** 544–50
- [6] Kusmartseva A F, Berger H, Forro L and Tutis E 2006 *Phys. Rev. Lett.* **103** 236401
- [7] Pyon S, Kudo K and Nohara M 2012 *J. Phys. Soc. Japan* **81** 053701
- [8] Kudo K, Ishii H, Takasuga M, Iba K, Nakano S, Kim J, Fujiwara A and Nohara M 2013 *J. Phys. Soc. Japan* **82** 063704

- [9] Núñez M, Freitas D C, Gay F, Marcus J, Strobel P, Aligia A A and Núñez-Regueiro M 2013 *Phys. Rev. B* **88** 245129
- [10] Freitas D C, Núñez M, Strobel P, Sulpice A, Weht R, Aligia A A and Núñez-Regueiro M 2013 *Phys. Rev. B* **87** 014420
- [11] Van Bruggen C F, Haange R J, Wieggers G A and De Boer D K G 1980 *Physica B* **99** 166–72
- [12] Bergerhoff G, Berndt M and Brandenburg K 1996 *Res. Natl Inst. Stand. Technol.* **101** 221
- [13] Harper J M E, Geballe T H and DiSalvo F J 1977 *Phys. Rev. B* **15** 2943
- [14] Hohenberg P and Kohn W 1964 *Phys. Rev. B* **136** 864
Kohn W and Sham L J 1965 *Phys. Rev.* **140** A1133
- [15] Blaha P, Schwarz K, Madsen G K H, Kvasnicka D and Luitz J 2001 *WIEN2K, An Augmented Plane Wave + Local Orbitals Program for Calculating Crystal Properties* (Vienna: Technische Universität Wien)
- [16] Perdew J P, Burke K and Ernzerhof M 1996 *Phys. Rev. Lett.* **77** 3865
- [17] Yuzuri M and Segi K 1977 *Physica B* **86–88** 891
- [18] Yuzuri M 1973 *J. Phys. Soc. Japan* **35** 1252
- [19] Ohta S, Narui Y and Sakayori Y 1997 *J. Magn. Magn. Mater.* **170** 168
- [20] Wontcheu J, Bensch W, Mankovsky S, Polesya S, Ebert H, Kremer R K and Bruecher E 2008 *J. Solid State Chem.* **181** 1492
- [21] Wontcheu J, Bensch W, Mankovsky S and Polesya S 2008 *Prog. Solid State Chem.* **37** 226
- [22] Huang Z-L, Bensch W, Benea D and Ebert H 2005 *J. Solid State Chem.* **178** 2778